ROMANIAN JOURNAL OF INFORMATION SCIENCE AND TECHNOLOGY
Volume **14**, Number 4, 2011, 365–379

Computation Models for Studying the Dynamic Behaviour of MEMS Structures. Determination of Silicon Dynamic Young's Modulus ($E_{dynamic}$)

Georgeta IONASCU[1], Adriana SANDU[2], Lucian BOGATU[1], Constantin Daniel COMEAGA[1], Elena MANEA[3], Daniel BESNEA[1]

[1]*Politehnica* University of Bucharest,
Department of Mechatronics and Precision Mechanics
[2]*Politehnica* University of Bucharest,
Department of Strength of Materials
[3]National Institute for Research & Development
in Microtechnology of Bucharest
E-mail: ionascu_georgeta@yahoo.com

Abstract. This paper presents a study on models of computation for predicting the vibration modes of a bulk-micromachined silicon accelerometer and structures of cantilever type – as suspension arms of the inertial mass of accelerometer, reported to the experimentally measured values of resonance (natural) frequencies. The values of silicon Young's modulus depending on the crystal orientation (isotropic and orthotropic silicon), of Bulk modulus and, also, of the dynamic Young's modulus determined by the authors, are considered. The aim of the paper is to find the most appropriate value of silicon elastic modulus that provides a precision of numerical simulation better than 5%, for the first natural (fundamental) frequency of a given MEMS structure.

Keywords: MEMS structure models, silicon microaccelerometer, resonance (natural) frequency, dynamic Young's modulus.

1. Introduction

During last decades, MEMS (Micro-Electro-Mechanical Systems) technology has been rapidly and successfully developed in achieving miniaturized mechanical structures and their integration with microelectronic components. Acceleration sensors have been amongst the first implemented MEMS products [1, 2, 3].

The mechanical properties of the materials used in MEMS fabrication are of great importance for designing the microdevices. These mechanical properties are strongly dependent on size, manufacturing processes of MEMS structures and crystal orientation in materials, due to anisotropy – preferred directions in the lattice of single crystalline materials, such as silicon wafers – the structural material chosen for the application under study.

Among the mechanical properties of interest, one can be mentioned the elastic properties (Young's modulus and Poisson's ratio) directly related to the device performance (mechanical behaviour). In the scientific literature [4], for silicon, the possible values of Young's modulus (E) range from 130 to 188 GPa, and that ones of Poisson's ratio (ν) between 0.048 and 0.4. The choice of the appropriate values for these material constants has a significant influence on the results of behaviour analysis of the MEMS structures.

Several testing methods using various test samples were developed [5, 6, 7], such as cantilevers or fully clamped bridges for determination of Young's modulus. They are based on the idea that it is essential to measure the mechanical properties of MEMS materials at the same size scale and to employ the same processes with those used in MEMS devices. Extraction of E by using these specimen types is possible from dynamic characteristics such as resonance frequencies. The resonance frequencies can be computed analytically for simple geometries like straight beams. In other cases, for multilayer structures or more complex shapes, the resonance frequencies can be computed using numerical simulations (Finite Element Method – FEM approach) for predicting, at the same time, the sensitivity and detection limits of these versatile micro devices [8].

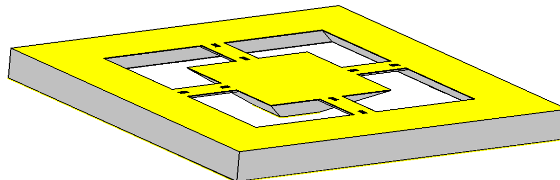

Fig. 1. 3D view of the piezoresistive microaccelerometer structure.

In this paper, in order to validate the precision of the finite element analysis, a comparative study on models of computation of the resonance frequencies for a bulk-micromachined silicon accelerometer (with releasing of mechanical structure through a wet anisotropic etching process on both sides of the silicon substrate), Fig. 1, as well as for the suspension arms of the inertial mass of accelerometer, is presented. The sensitive elements (piezoresistors) are diffused into the suspension arms, nearly the rim

and the inertial mass, on perpendicular directions, Fig. 2. (100) silicon wafers were patterned so that the edges of the suspension arms were in the $< 110 >$ directions.

In the analytical calculations, the suspension arms were modeled as cantilever beams and cantilever rectangular plates. Values of E, for both isotropic and orthotropic silicon, were considered. The Bulk modulus (B) was considered too, based on the experimental study through which the actual dynamic Young's modulus ($E_{dynamic}$) was determined. The resonance (natural) frequencies of both accelerometer and cantilevers, detached together with the rim from the accelerometer structure, were measured using MSA-500 Micro System Analyzer (Polytec).

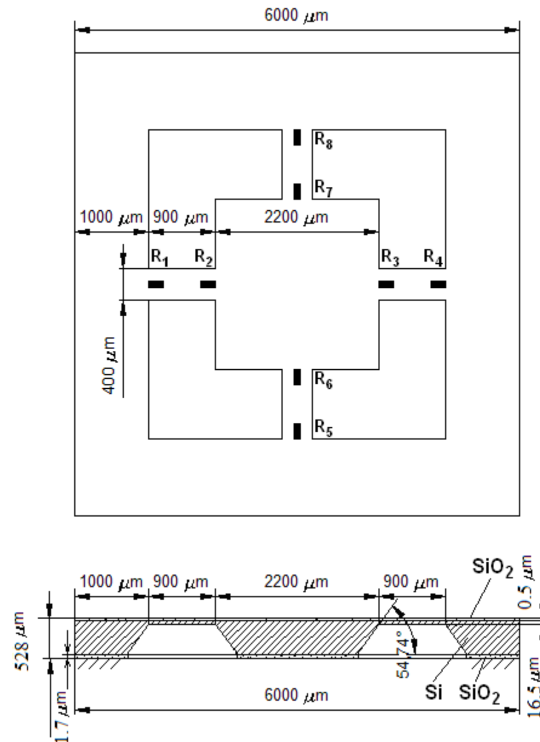

Fig. 2. Components and sizes of the analysed structure, and piezoresistor positioning on the suspension arms (overall dimensions of piezoresistors: w_p(width)∼70μm, l_p(length)∼140 μm, d_p(depth of diffusion)∼2 μm).

2. Theoretical considerations

The resonance frequencies for homogeneous (silicon) cantilever beams and rectangular plates are computed with the expressions given in (1) and (2) – (3), respectively [9, 10]:

$$f_i = \frac{n_i^2}{2\pi l^2}\sqrt{\frac{EI}{\rho A}}, \tag{1}$$

where: EI – the bending stiffness: l, A – the length and cross-sectional area of the beam; ρ – the density of the beam material; n_i – coefficients with specified values corresponding to the vibration modes.

$$f_i = \frac{\alpha_i}{2\pi}\sqrt{\frac{D}{\rho h l^4}}, \tag{2}$$

$$D = \frac{Eh^3}{12\left(1-\nu^2\right)}, \tag{3}$$

where: l, h – the length and thickness of the plate; E, ν, ρ – the Young's modulus, Poisson's ratio and density of the plate material; α_i – computed coefficients based on length (l)/width (b) ratio corresponding to the vibration modes.

For non-homogeneous (oxide-coated silicon) structures modeled as cantilever beams, the bending stiffness EI and density ρ are replaced in equation (1) with the composite bending stiffness $\overline{EI}$ and composite density $\overline{\rho}$ [8]:

$$\overline{EI} = \sum_{j=1}^{N} E_j I_j, \tag{4}$$

$$\overline{\rho} = \frac{\sum_{j=1}^{N} \rho_j h_j}{\sum_{j=1}^{N} h_j}, \tag{5}$$

where: N – the number of layers in the composite cantilever, $E_j I_j$ – the bending stiffness of the individual layers, ρ_j – the density of the individual layers, h_j – the thickness of the individual layers.

The position, the dimensions and materials of the cantilevers are shown in Fig. 3 and Table 1.

Table 1. Dimensions of cantilevers

Cantilever position	***l* (μm)**	***b* (μm)**	***h* (μm)**
1	877	409.5	17
2	944.5	408	
3	870	411	

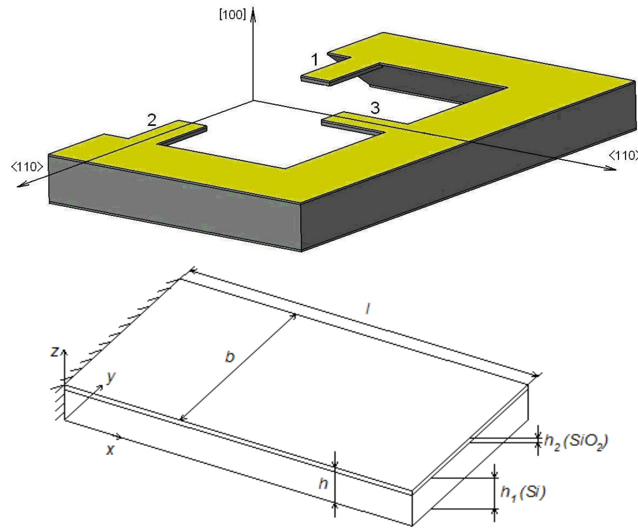

Fig. 3. Scheme of cantilevers used in out-of-plane vibration test.

3. Experimental procedure. Determination of silicon dynamic Young's modulus

As etch and boron diffusion (for piezoresistors) mask, a thermally grown oxide was used. The inertial mass is shaped like a truncated pyramid due to the anisotropic etchant (KOH) which exposed the {111} planes. The patterning mask was provided with compensation structures to avoid convex corner undercut of the inertial mass. In absence of an etch stop layer, etching time was estimated to create the required cantilever thickness and inertial mass height. The obtained structure of microaccelerometer is shown in Fig. 4.

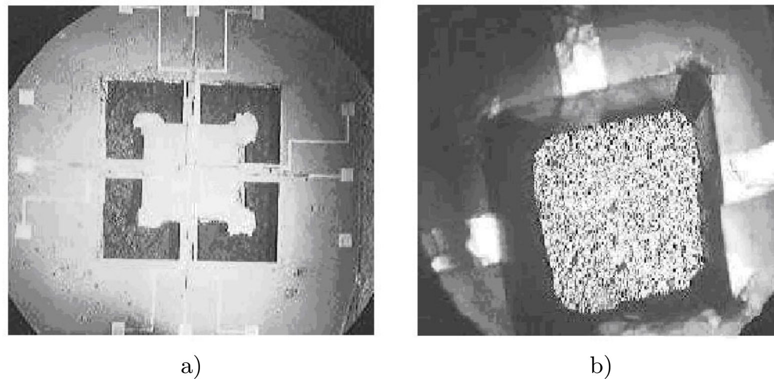

a) b)

Fig. 4. Photos of the microaccelerometer structure: front view (a) and the inertial mass (b).

In order to characterize the geometry and the dynamic behaviour of structures, the MSA-500 Micro System Analyzer was used, Fig. 5.

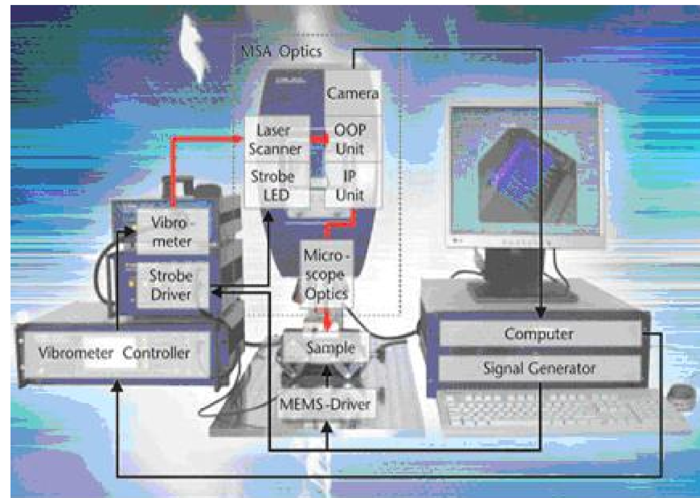

Fig. 5. Schematic representation of the MSA.

It has a unique combination of non-contact measurement techniques: Scanning Laser-Doppler Vibrometry for characterization of out-of-plane vibrations; Stroboscopic Video Microscopy for measurement of in-plane motion and vibration; White Light Interferometry (WLI) for determination of surface topography; Geometry Scan data acquisition for the vibration measurement [11, 12].

The Laser-Doppler Vibrometer (LDV) is a very precise optical transducer for determining the vibration velocity and displacement in a sample point. It works by sensing the frequency shift of back scattered light from a moving surface. By moving the measurement point to predefined positions, a Scanning LDV provides the full picture of a device's out-of-plane vibrational behaviour. There are no discrete frequencies at which measurements must be performed. Frequency data over the instrument bandwidth are available within milliseconds per sample point.

The measurements were made on individual chips bonded through the structure rim onto a metal rigid plate of $12 \times 12 \times 5$ mm^3. The plate there is fixed through an elastic double adhesive layer on a piezoelectric excitator consisting of a multilayer ceramics piezoelectric actuator mounted in an elastic pre-tensioned housing. The equipment has two laser beams whose signals are optically subtracted in the interferometer. The first (reference) beam can be positioned manually (using software) in the visual field of microscope, while the second (measuring) beam is automatically moved in the points of a scanning grid defined by the user, Fig. 6.

During measurement, the reference beam is fixed at a point on the structure rim, and the other one remains mobile. So, only the vibration of the structure points relative to the rim is measured. This manner of differential measurement avoids the influence of excitator dynamics on the determinations for the analyzed structure.

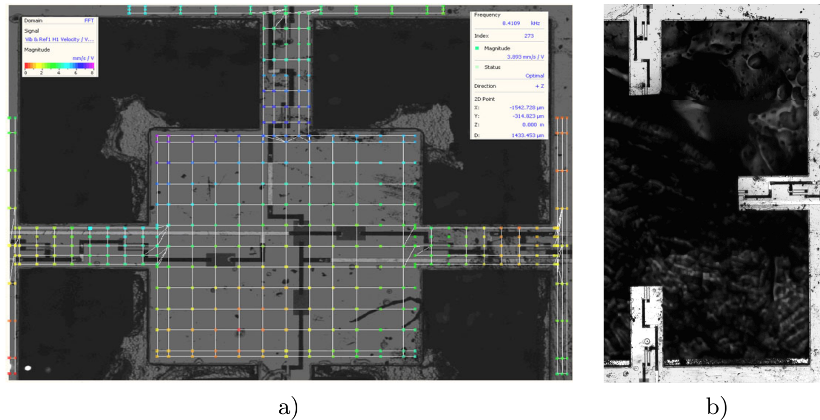

a) b)

Fig. 6. Images of the tested structures on MSA: accelerometer with a scanning grid (a) and the suspension arms/cantilevers after the detachment of the inertial mass (b).

Every point, test was performed by using a sinusoidal signal applied to the piezoelectric excitator. The signal was varied in a domain of frequency ranged from 0.5 up to 150 kHz, with 6400 measuring intervals. For the low-frequency modes, the resolution in the detection of natural frequencies has been improved by limiting the frequency of testing at 10 kHz. (Observation: at high frequencies, signal to noise ratio is very low, and accuracy in identifying the natural frequencies is reduced).

The average spectrum of transfer function between velocity response and the testing signal over the entire structure of accelerometer is presented in Fig. 7.

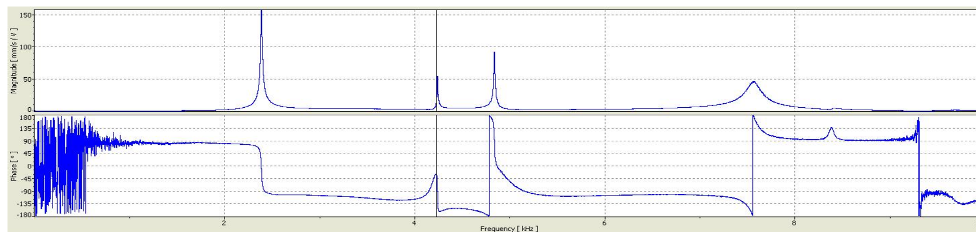

Fig. 7. Spectrum of response of the vibration velocity.

After measuring, significant differences between the similar modes of vibration (2-3) were found. Due to the structure symmetry of accelerometer, they would be equal or very close. These differences can be explained by various behaviours of the four suspension arms due to the technological execution errors and the material anisotropy. Consequently, the domain of frequency analysis was broadened in order to study the microcantilevers and to determine the dynamic Young's modulus ($E_{dynamic}$) of silicon.

The measured resonance frequencies for the tested cantilevers are listed in Table 2. The values of the measured resonance frequencies were introduced in the equations (1) and (2), for suspension arms of dimensions given in Table 1. The material data used in computation were: $\rho_{Si} = 2330$ kg/m^3, $\nu_{Si} = 0.22$ (the structures were considered homogeneous, made from silicon as an isotropic material). The obtained average

values for $E_{dynamic}$ in the two cases, beam model and plate model, are given in Table 3. The values $E_{dynamic}$ (beam model) = 103.9 GPa and $E_{dynamic}$ (plate model) = 90.6 GPa have resulted lower than Young's modulus from (100) crystalline plane of silicon $E_{(100)}$ = 130 GPa, but close to silicon Bulk modulus B = 97.8 GPa [4], validating the models of analytical and numerical computation presented below.

Table 2. The resonance frequencies measured on the cantilever structures using MSA-500

Vibration mode	**Cantilever position**	**Resonance frequency, f (kHz) – average values**
1 (bending)	1	22.852
	2	20.885
	3	20.654
2 (torsion)	1	96.289
	2	92.682
	3	93.291
3 (bending)	1	148.378
	2	142.142
	3	143.330
4 (torsion)	1	321.269
	2	313.014
	3	318.047
5 (bending)	1	420.839
	2	409.648
	3	408.964

Table 3. Dynamic Young's modulus of silicon, extracted from analytical models using the experimentally determined resonance frequencies

$E_{dynamic}$(GPa), beam model	**$E_{dynamic}$(GPa), plate model**
103.9	90.6

4. Analytical models (AM) and numerical models (FEM) of computation for cantilever structures

In the case of homogeneous model, the structures are made entirely from silicon (h = 17 μm), neglecting the oxide layer. The non-homogeneous model corresponds to the actual structures made from oxide-coated silicon (Fig. 3), where $h_{1(Si)}$ = 16.5 μm and $h_{2(SiO_2)}$ = 0.5 μm. For each structure type, different values of elastic constants of silicon were taken into account depending on the crystal orientation [4], summarized in Table 4.

Table 4. Elastic constants of isotropic silicon

Elastic modulus	$E_x = E_y = E_z$ = 130 GPa (E_{100})	B = 97.8 GPa
Poisson's ratio	$\nu_{yz} = \nu_{zx} = \nu_{xy} = 0.28$	$\nu = 0.28$

In all cases, density $\rho_{Si} = 2330$ kg/m^3. The oxide layer was modeled as an isotropic material, with $E_{SiO_2} = 70$ GPa, $\nu_{SiO_2} = 0.17$ and $\rho_{SiO_2} = 2200$ kg/m^3.

Six analytical models were developed, Table 5.

Table 5. Analytical models

Homogeneous structure	**Non-homogeneous structure**
AM_beam_Si iso_E$_{100}$_1	AM_beam_Si iso_E$_{100}$_2
AM_beam_Si iso_B_1	AM_beam_Si iso_B_2
AM_plate_Si iso_E$_{100}$_1	
AM_plate_Si iso_B_1	

By employing the COSMOS/M - GeoSTAR software attached to SolidWorks programming medium, numerical models of simulation were performed for the structures given in Fig. 3. For microstructures, an optimum must be found between a finer mesh and the computation accuracy required for the natural frequency determination. 7500 elements of 3D SOLID interconnected in 9486 nodes were used. The modeling was made both for isotropic silicon and orthotropic silicon, which corresponds to the actual structures. The values of elastic constants of the orthotropic silicon are given in Table 6 [4].

Table 6. Elastic constants of orthotropic silicon

Elastic modulus	$E_x = E_y = 169$ GPa (E_{110}) $E_z = 130$ GPa (E_{100})
Poisson's ratio	$\nu_{yz} = 0.36$, $\nu_{zx} = 0.28$, $\nu_{xy} = 0.064$

Five numerical models were developed, Table 7.

Table 7. Numerical models

Homogeneous structure	**Non-homogeneous structure**
FEM_Si iso_E$_{100}$_1	FEM_Si iso_E$_{100}$_2
FEM_Si ortho_1	FEM_Si ortho_2
	FEM_Si iso_B_2

The shape of the first five vibrations modes, computed with FEM and experimentally determined using MSA is presented in Fig. 8.

A comparison between the analytical and numerical models, of homogeneous and non-homogeneous structure, for the first (fundamental) vibration mode and for all the five modes, reported to the experimentally measured resonance frequencies, is presented in Figures 9, 10, 11 and Fig. 12, respectively.

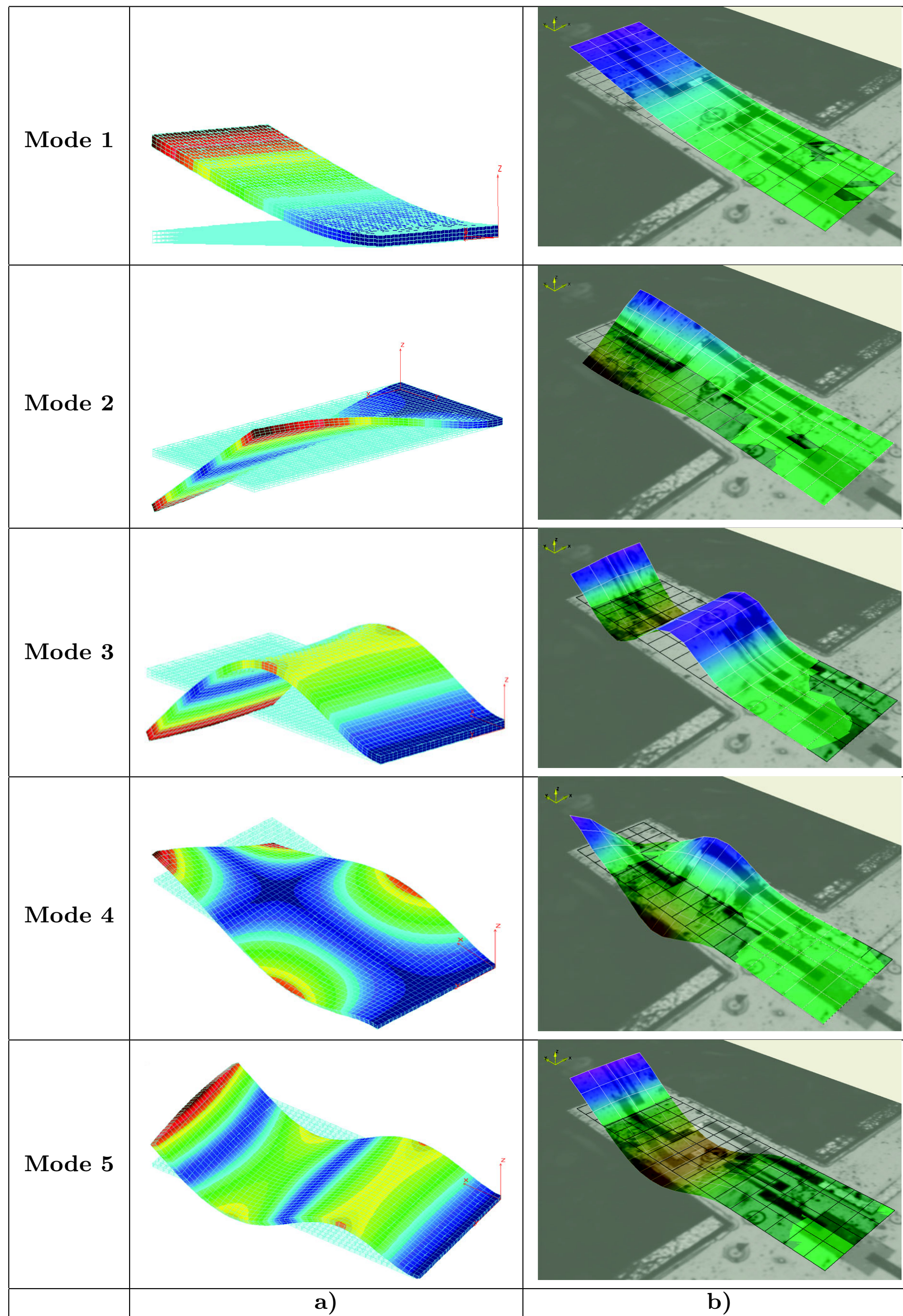

Fig. 8. Shape of the first five vibration modes for cantilever structures: computed with FEM (a) and experimentally determined using MSA (b).

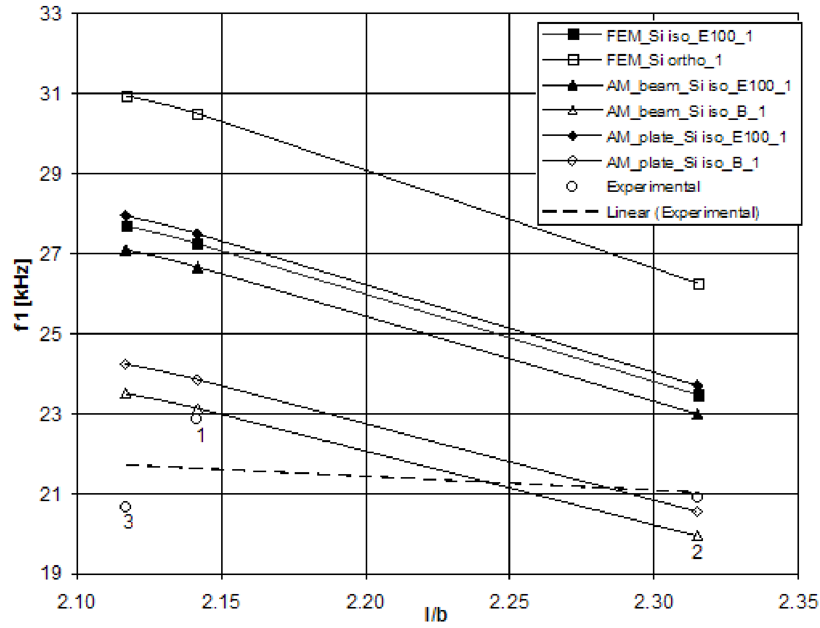

Fig. 9. Comparison between analytical and numerical models for the first mode – homogeneous structure; 1, 2, 3 cantilever position.

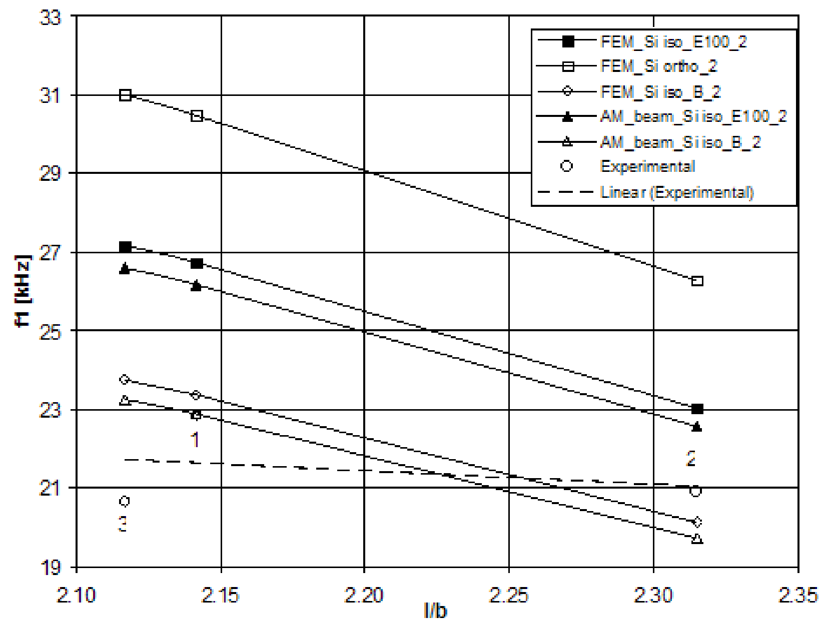

Fig. 10. Comparison between analytical and numerical models for the first mode – non-homogeneous structure; 1, 2, 3 cantilever position.

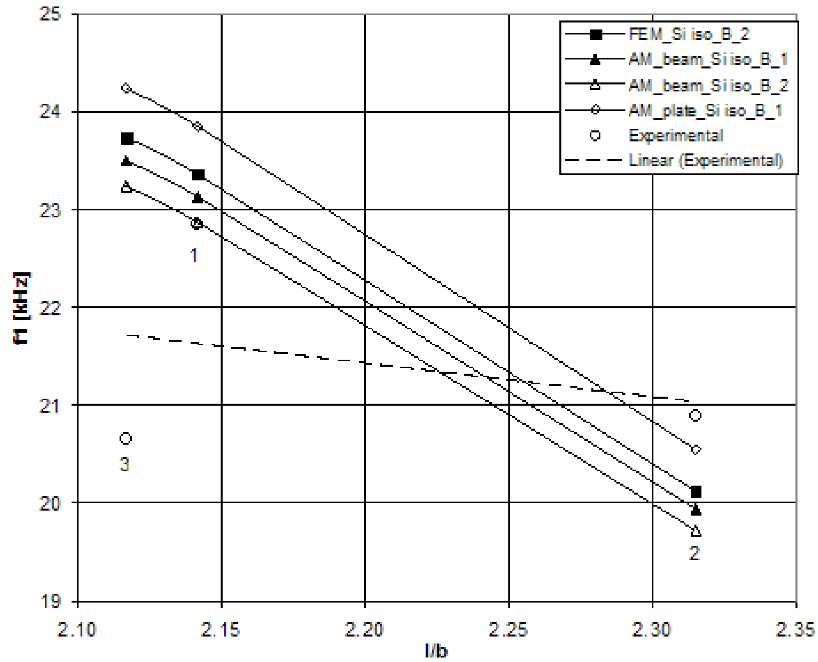

Fig. 11. Comparison between analytical and numerical models for the first mode – homogeneous and non-homogeneous structures, computed with Bulk modulus (B); 1, 2, 3 cantilever position.

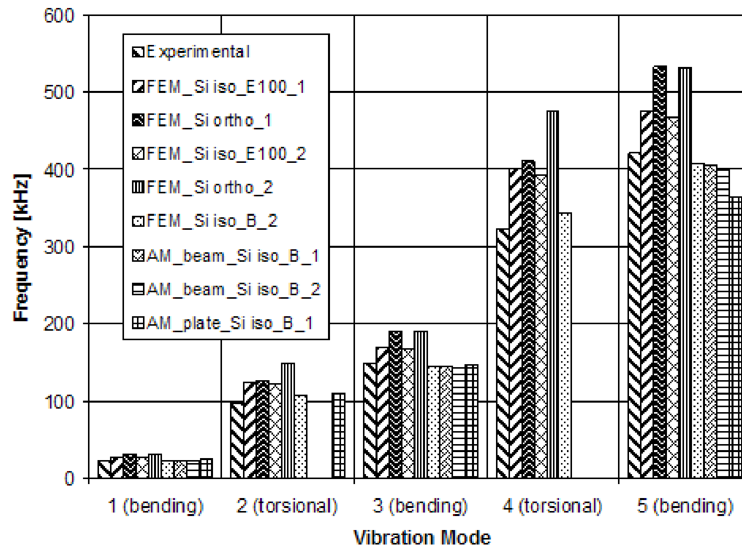

Fig. 12. Comparison between analytical and numerical models for all the five vibrations modes.

5. Validation of numerical simulation for dynamic behaviour of MEMS accelerometer structure

For the ideal structure of accelerometer (Fig. 2), considering it entirely made from silicon, as an isotropic model, a numerical simulation was performed by means of COSMOS/M software package using 9600 elements of 3D solid interconnected in 12573 nodes. The shape of the first three vibrations modes computed with FEM and experimentally determined using MSA is presented in Fig. 13.

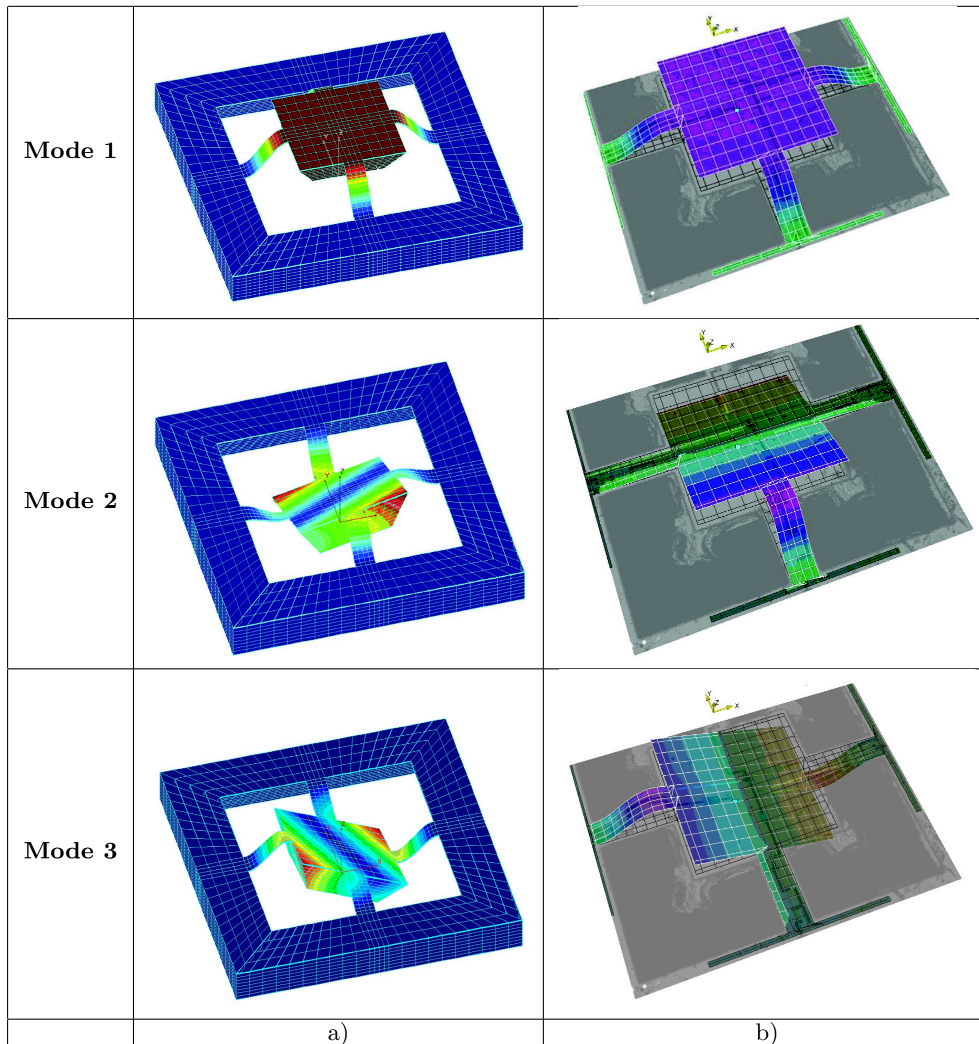

Fig. 13. Shape of the first three vibration modes for accelerometer structure: computed with FEM (a) and experimentally determined using MSA (b).

The natural frequencies from the first to the third vibration mode, obtained by FEM in two cases – for $E_{(100)}$ and B values and compared with the resonance frequencies measured with MSA-500 Analyzer, are given in Table 8.

Table 8. The first three vibration modes of the accelerometer structure, experimentally determined and computed with FEM

Vibration mode	f (Hz) measured with MSA-500 Analyzer	FEM with $E_{(100)} = 130$ GPa		FEM with $B = 97.8$ GPa	
		f (Hz)	Deviation (%)	f (Hz)	Deviation (%)
1	2384.4	2854.6	19.7	2494.3	**4.6**
2	4232.8	5250	16.3 (average value)	4587	6.7 (average value)
3	4836.7	5250		4587	

6. Discussion and conclusions

- The analytical models of homogeneous and non-homogeneous beam lead to values of resonance frequencies very close between them, whose precision reported to the experimental values is dependent on the elastic modulus of silicon. A good agreement is for B value.
- The homogeneous model of plate, even though is based on some approximations, is enough good for the first three natural frequencies and sufficiently precise for f5. Big errors were obtained for the fourth (torsional) mode. A good agreement is, also, obtained for B value.
- In all cases, the theoretical values of resonance frequencies are higher than those experimentally determined. The numerical computation has the advantage that can be modeled the actual structure, a layered composite structure. Both thin oxide layer and silicon substrate were modeled as isotropic materials, considering for silicon elastic modulus the B value, which is the closest value to $E_{dynamic}$ value.
- A detailed computation considering the orthotropic behaviour of silicon leads to correct results only if one can choose local coordinates, which coincide with those of crystal orientation (if they are known).
- The analytical models of computation have allowed by using the experimentally measured natural frequencies to determine the dynamic Young's modulus of silicon (for homogeneous structure). The value of Bulk modulus is very close to the values of $E_{dynamic}$, for any model (beam or plate). That's why for such analysis, in this paper, a very good precision was found when B value was considered.
- Concerning the accelerometer structure, the lowest deviations have been obtained (**4.6%** in the case of fundamental mode) for the numerically computed values of the resonance frequencies using, also, the B value.

Finally, for the dynamic analysis of MEMS structures, simple analytical models or numerical simulations by FEM can be used, but the precision of results (values of natural frequencies) highly depends on the value of the silicon elastic modulus.

Further research will continue to develop numerical analyses by FEM in correlation with experimental tests for identifying the most appropriate models, which describe the mechanical properties of silicon from MEMS structures related to the manufacturing technology and the loading type.

Acknowledgements. This work was funded by the Executive Unit for Financing Higher Education, Research, Development and Innovation (UEFISCDI) from the Contract of scientific research no. 72-187/1.10.2008. "Research and development of ultra high-tech (micro)mechatronic (micro)systems, integrated in technological platforms for upgrading and European qualification of the industry".

References

[1] Ionascu G., *Technologies of Microtechnics for MEMS* (in Romanian), Cartea Universitara Publishing House, Bucharest, 2004.

[2] Zha X. F., *Database System for Design and Manufacturing of MEMS*, Int. Journal of Adv. Manuf. Technol., **32**, p. 378, 2007.

[3] Ferrari V., Ghisla A., Marioli D., Taroni A., *MEMS Accelerometer with Multiaxial Response by Dynamic Reconfiguration of Piezoresistive Bridges*, Proc. of Eurosensors XX Conference, Göteborg, Sweden, M2B-P18, September 2006.

[4] Hopcroft M. A., Nix W. D., Kenny T. W., *What is the Young's Modulus of Silicon?*, J. Microelectromech. S., **19**, p. 229, 2010.

[5] Kamat S. V., *Mechanical Properties in MEMS*, DRDO Science Spectrum, p. 203, March 2009.

[6] Stanimirovic Z., Stanimirovic I., *Mechanical Properties of MEMS Materials*, Kenichi Takahata (Ed.), InTech, p. 165, Croatia, 2009.

[7] McShane G. J., Boutchich M., Srikantha Phani A., Moore D. F., Lu T. J., *Young's Modulus Measurement of Thin-Film Materials Using Micro-Cantilevers*, J. Micromech. Microeng., **16**, p. 1926, 2006.

[8] Ionascu G., Bogatu L., Sandu A., Manea E., Cernica I., *Modeling, Simulation and Technology of Microbeam Structures for Microsensor Applications*, UPB Scientific Bulletin, Series D, **70**, p. 19, 2008.

[9] Rades M., *Mechanical Vibrations*, Printech Publishing House, p. 264, Bucharest, 2006.

[10] Voinea R., Voiculescu D., Simion F. P., *Introduction to solid mechanics with applications in engineering* (in Romanian), Publishing House of Romanian Academy, p. 863, Bucharest, 1989.

[11] Ozdoganlar O.B., Hansche B.D., Carne T. G., *Experimental Modal Analysis for Microsystems*, Proc. Of IMAC-XXI Conference & Exposition on Structural Dynamics, 2003.

[12] Comeaga C. D., Alionte C. G., *Testing Methods for the Dynamics of Microstructures*, Proc. of International Symposium AVMS'2009 – Timisoara, p. 120, May 2009.